Model-based optimization of wind farms with Extremum seeking control

1st Eiríkur Ingi Jónsson
Reykjavík University

2nd Elias August
Reykjavík University

***Abstract*—The performance of a wind farm can be greatly increased with wake steering [1]. This report looks into utilizing extremum seeking control k a better control scheme for wind farms that takes into account the total energy production.**

I. Introduction

The generation of electricity from wind energy has seen a dramatic rise in the last two decades [2]. This rise has been driven in part by the need for a renewable and sustainable substitute for greenhouse gas emitting fossil fuels, with many countries looking towards wind energy to meet the Paris agreement [3].

Wind energy

The instantaneous power available for extraction from wind depends on the mass flow of air particles, $\dot{m}$, and the wind speed, U,

$$P_{wind}(U) = \frac{1}{2}\dot{m}U^2 = \frac{1}{2}A\rho U^3. \tag{1}$$

Here, ρ is the air density and A represents the area of an imaginary surface. In this report this surface is the disc **created** by the spinning blades of a turbine.

The energy extraction of a turbine affects the behaviour of the wind downstream from it, decreasing wind speed and increasing turbulence. Due to the strong relationship between the wind speed and power production, optimising turbine attitudes to decrease the wake effect can have great benefits [1]. The aim of this paper is to achieve these benefits in a simple wind farm model. To that end, we consider an objective function that is the sum of the power produced by the individual turbines in the farm,

$$J(\gamma, v_i) = \sum_{i=1}^{n} P_i(\gamma_i, v_i), \tag{2}$$

where n is the number of turbines and P_i represents the power produced by a single turbine. It is a function of the wind at its rotor, v_i, and the yaw angle, γ_i, i.e. the angle between the wind direction and the rotor rotation axis, and is given by

$$P_i(\gamma_i, v_i) = C_p(\gamma_i)P_{wind}(v_i). \tag{3}$$

C_p is the power coefficient of the turbine [4], which determines how much of the available energy the turbine is able to extract,

$$C_p(\gamma) = \frac{16}{27}cos(\gamma)^{1.88}. \tag{4}$$

With a yaw angle of zero, a turbine operates at the Betz limit, $\frac{16}{27}$, the theoretical maximum ratio of power that a turbine can extract from the wind [5].

Jensen wake model

The Jensen wake model [6] was first introduced in 1983, offering a simple way to model the wind speed in the wake of a turbine. The Jensen model assumes a linear expansion of the wake with a starting diameter being the turbine diameter. The wake diameter at a distance X downwind from a turbine is given as

$$R_W(X) = R + kX, \tag{5}$$

where R is the radius, or blade length, of the turbine and k is the wake area expansion rate, set to 0.04. This is shown in Fig. 1.

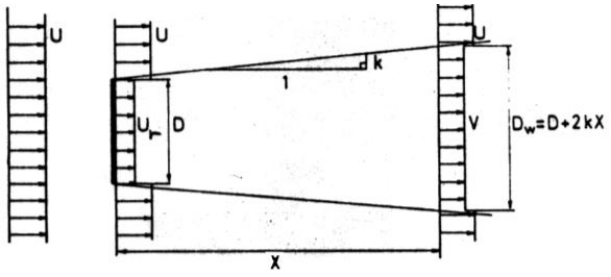

Figure 1: The wake expansion of the Jensen wake model [7].

The wind velocity at a turbine in the wake of another is given by

$$v(X) = U\left(1 - \frac{2/3}{\left(1 + \frac{kX}{R}\right)^2}\frac{A_{overlap}}{\pi R^2}\right), \tag{6}$$

where $A_{overlap}$ is the area of the virtual rotor disc affected by the wake, as seen in Fig. 2.

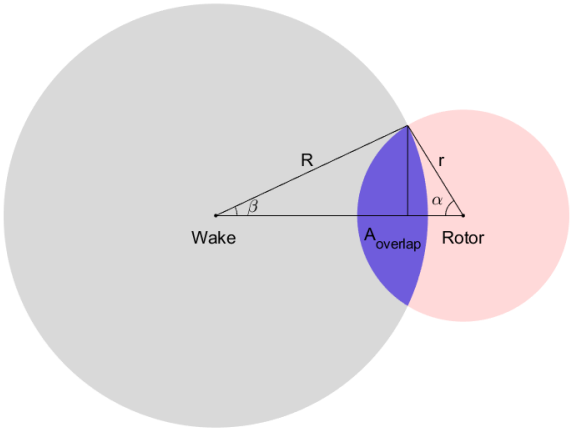

Figure 2: The overlapping area, blue, between the wake disc, gray, and the rotor disc, red.

From geometry, the overlapping area is given by

$$A_{overlap} = \begin{cases} r^2\pi & \text{if } d < R - r \\ 0 & \text{if } d \geq R + r \\ r^2\left(\alpha - \frac{sin(2\alpha)}{2}\right) + & \\ R^2\left(\beta - \frac{sin(2\beta)}{2}\right) & \text{otherwise} \end{cases} \tag{7}$$

Here, d is the distance between the centres of the circles, R is the wake diameter, r is the rotor diameter and α and β are the angles shown in Fig. 2,

$$\alpha = \arccos\frac{d^2 + r^2 - R^2}{2dr}, \ \beta = \arccos\frac{d^2 + R^2 - r^2}{2dR}. \tag{8}$$

The distance between the centers is given by

$$d = |(x_2 - x_1)\tan\gamma_1 + y_1 - y_2|, \tag{9}$$

where $[x_1, y_1]$ and $[x_2, y_2]$ are the coordinates of the upstream and downstream turbines, respectively (see Fig. 3).

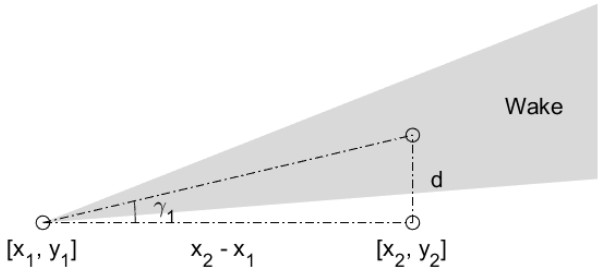

Figure 3: Illustration of wake geometry.

The combined wake effect of multiple turbines is given by the sum of squares of the velocity deficits [7],

$$\left(\frac{v(X)}{U}\right)^2 = \sum\left(1 - \frac{v_i(X)}{U}\right)^2, \tag{10}$$

where v_i is the velocity at the wake of an upstream turbine indexed by i.

II. Example

Consider a wind farm with 2 turbines, one positioned directly downstream of the other at distance $4D$. As yawing the downstream turbine will only reduce power, we keep its yaw angle at zero. Thus, only the yaw angle of the upstream turbine is of interest and considered the free variable of the optimisation problem. The total power generated by the wind farm is given by

$$J(\gamma_1) = \frac{1}{2}A\rho U^3 \times \left(C_p(\gamma_1) + C_p(0)\left(1 - \frac{2/3}{\left(1 + \frac{k(x_2)}{R}\right)^2}\frac{A_{overlap}(\gamma_1)}{\pi R^2}\right)^3\right). \tag{11}$$

This is illustrated in figure 4.

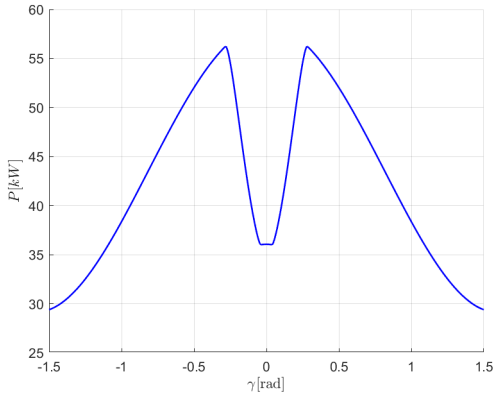

Figure 4: Total power generation as a function of the yaw angle of the upstream turbine. The two peaks observed correspond to angles where the downstream turbine escapes the wake.

As eq. 7 is discontinuous, the maximas of eq. 11 can not be found from its derivative alone. In fact, the maximas lie at points of no wake overlap for the downstream turbine and the least yaw misalignment for the upstream turbine, i.e. $d = R+r$. Substituting eq. 9 yields $\gamma_1 = \arctan\frac{2r+kx_2}{x_2} = \pm 0.282\ rad$

However, in reality, the relationship between wind farm power production and the yaw angles of the different wind turbines is much more complicated than the one depicted in Fig. 4 and difficult to model. Thus, let us assume that a relationship given by Eq. 11 is not available to us. Instead, we consider *extremum seeking control (ESC)* to search for a yaw angle that provides optimal power production. ESC is a model-free optimisation approach that can use measurements only to estimate the gradient of an objective function to follow in order to find its maximum or minimum [8].

Particularly, in this example, we continuously perturb the yaw angle of the upstream turbine slightly. The rationale for finding a power maximum is the following. If increasing/decreasing the yaw angle increases/decreases power then

the former shall be increased. If power does the opposite when the yaw angle increases/decreases than it shall be decreased. The approach we employ to achieve this rationale, while keeping the angle between $\pm\frac{\pi}{2}$, is given by

$$\begin{aligned} \dot{\hat{\gamma}} &= k_2 \dot{J} sin(\omega t), \\ \gamma &= \hat{\gamma} + k_1 sin(\omega t), \\ \dot{J}(\gamma_1) &= \frac{dJ(\gamma_1)}{d\gamma_1}\dot{\gamma}_1. \end{aligned} \tag{12}$$

Let $D = 20m$, $U = 8\frac{m}{s}$, $k = 0.04$, $\rho = 0.6125\frac{kg}{m^3}$, $k_1 = 0.05\ rad$, $k_2 = 5 \times 10^{-6} W^{-1}$, and $\omega = 10\pi\frac{rad}{s}$. Figure 5 shows how the yaw angle of the upstream turbine changes with respect to time. The initial yaw angle of the upstream turbine is set to zero, i.e. $\gamma_1(0) = 0$ rad. Figure 6 shows the changes

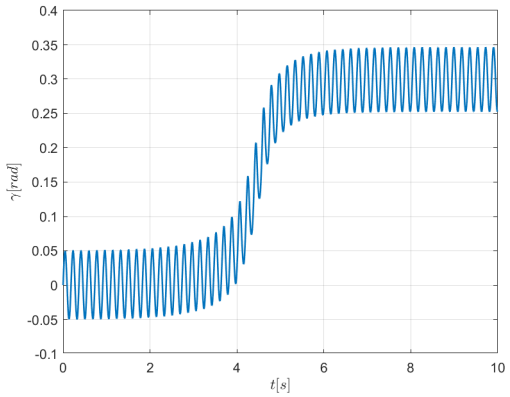

Figure 5: Changes in yaw angle of upstream turbine over time.

in power with respect to time, corresponding to the changes in γ_1. Observe that as γ_1 deviates from zero, P_1 decreases. This corresponds to a decrease in its power coefficient. Conversely, the downstream turbine experiences an increase in velocity as it is cleared from the wake, leading to an increase in P_2 and a net increase in power output.

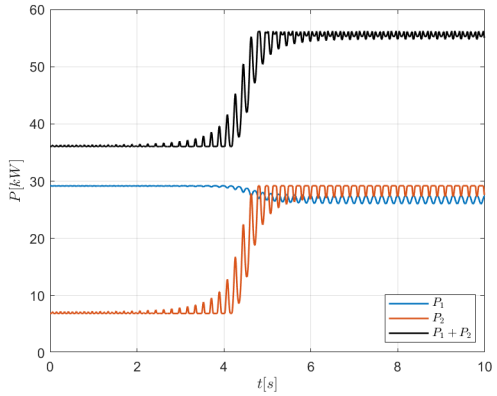

Figure 6: Changes in power generation over time. The black line represents the objective function, eq. 2.

III. FLORIS

In this section we will attempt to recreate the results of section II using the *FLOw Redirection and Induction in Steady State (FLORIS)* tool [9]. FLORIS is a wind plant modeling tool, widely used for optimization purposes. FLORIS was developed by the National Renewable Energy Laboratory(NREL) and the Delft University of technology.
Let us again consider a 2-turbine wind farm, with a distance of $4D$ between the turbines. Setting a constant yaw angle of 0 for the downstream turbine and sweeping the upstream turbine from $-45°$ to $45°$ produces two peaks as seen in figure 7.

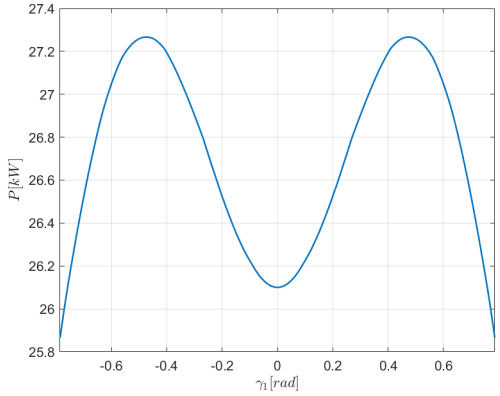

Figure 7: Total power as a function of γ_1.

Figures 8-10 show the wake profiles corresponding to the peaks in figure 7.

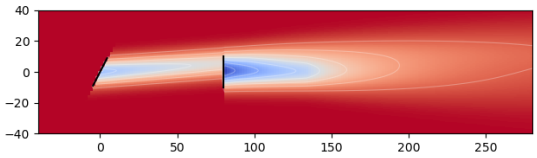

Figure 8: Wind velocity profile for $\gamma_1 \approx -0.5rad$.

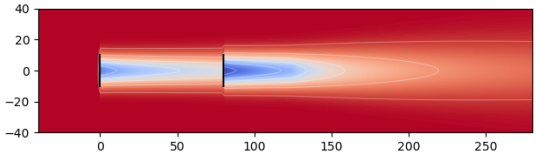

Figure 9: Wind velocity profile for $\gamma_1 = 0rad$.

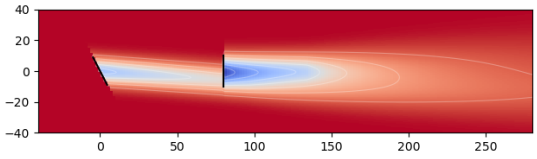

Figure 10: Wind velocity profile for $\gamma_1 \approx 0.5rad$.

Again, we employ ESC to find the optimal yaw angle. Let $D = 20m$, $U = 8\frac{m}{s}$, $\rho = 0.6125\frac{kg}{m^3}$, $k_1 = 0.05rad$, $k_2 = 0.25W^{-1}$, and $\omega = 20\pi\frac{rad}{s}$. The simulation parameters of the wind farm and turbines remain unchanged from the

previous section; however, due to a difference in power calculations between models, the optimization parameters must be changed. Figure 11 shows how the yaw angle of the upstream turbine changes with respect to time.

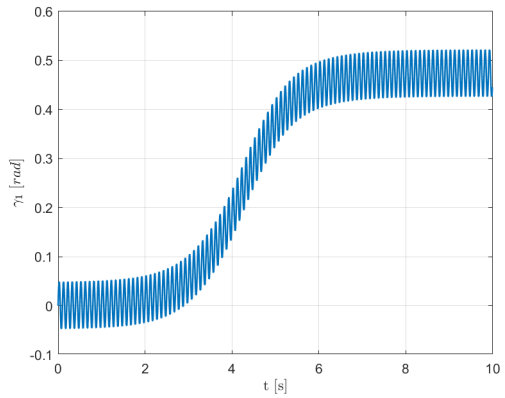

Figure 11: Changes in γ_1 over time.

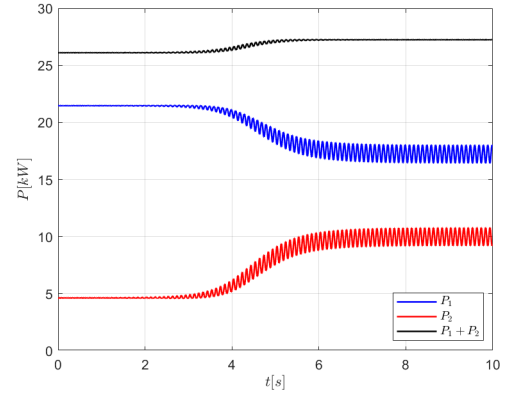

Figure 12: Changes in power generation over time.

Clearly, these results agree with the results from section II.

IV. Results

One interesting finding is when three or more turbines are arranged in a row configuration, with the row being parallel to the wind direction. In this case yawing all upstream turbines to the same side yields better results than other alignments, e.g. alternating yaw alignments. This is illustrated with three turbines in figures 13-14.

Observe that the wake from the upstream turbines covers a larger area of the last turbine with the alternating alignment. The upstream turbines are also affected, as shown in table I.

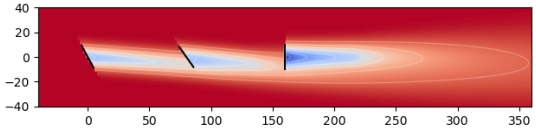

Figure 13: Same side yaw alignment.

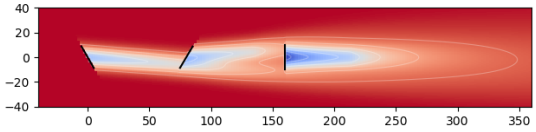

Figure 14: Alternating yaw alignment.

Table I: Comparison of same side- and alternating yaw alignment for a wind farm of three turbines. The third column shows the difference between absolute values of the same side and alternating cases.

Case	Same side	Alternating
γ_1 $[rad]$	0.50	0.52
γ_2 $[rad]$	0.62	-0.54
γ_3 $[rad]$	0	0
P_1 $[kW]$	16.90	16.42
P_2 $[kW]$	6.85	8.02
P_3 $[kW]$	12.44	10.59
P_T $[kW]$	36.19	35.03

Figure 15 shows the comparison of the total power output of these cases.

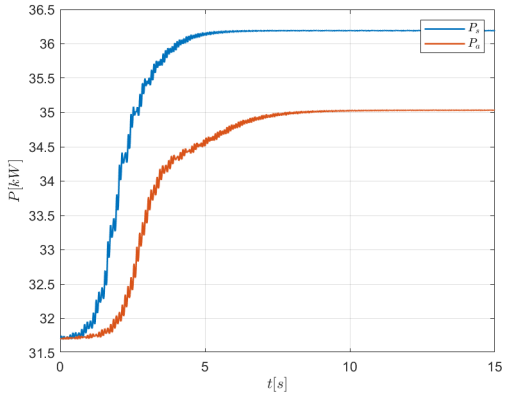

Figure 15: Power output for same side(blue) vs. alternating(red) yaw alignments.

This difference becomes greater with more turbines.
To achieve the alternating yaw alignment, a small negative initial yaw angle was set for the second turbine. As ESC essentially works as a gradient descent algorithm, it does not guarantee convergence to global optima in every case. However, it rarely converges to the alternating yaw alignment and only does so when the frequencies of the first and second turbines are very similar.

Different wind directions

So far we've focused on wind farms in a stream-wise row configuration, but that is clearly a rare situation. Figures 16 and 17 show how 2 different wind farms, of common configurations, may benefit from wake steering, depending on the direction of the wind.
A wind direction of 270 represents a east-to-west direction, as shown in figures 8-10 and 13-14.
To produce figures 16 and 17, an initial angle of $0rad$ is set for all turbines and ESC is performed for 50 seconds. The initial power is used as a baseline for the gain calculations,

$$G = 100 \cdot \frac{P_f - P_i}{P_i}, \tag{13}$$

where P_f and P_i are the final and initial power output values, respectively.

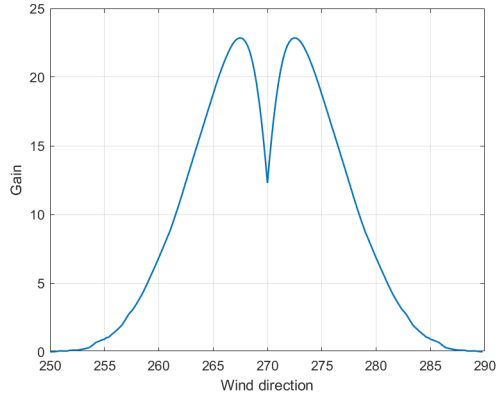

Figure 16: Gain vs wind direction for a 5 turbine wind farm with a row configuration.

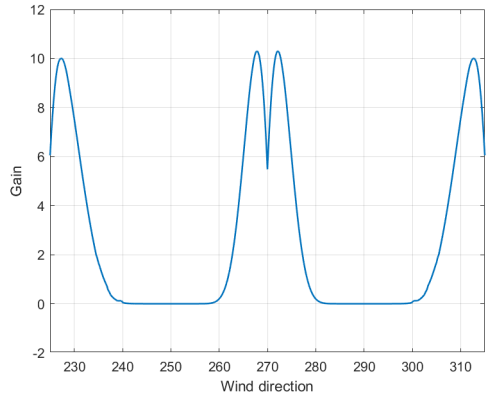

Figure 17: Gain vs wind direction for a 5 turbine wind farm with a rectangular grid configuration with one turbine position in the center. The outer turbines have a distance of $7D$ between them.

V. Wake model comparison

In this section we will compare the effect of ESC on a few of the wake models available within the FLORIS software. This comparison will be made by optimizing a wind farm consisting of 3 turbines in a row configuration with a distance of $7D$ between turbines. 4 models will be used for the comparison. These models are called *Gauss* [10]–[15], *Gauss legacy* [10]–[14], *Gauss-Curl hybrid* [16] and *Blondel* [15]. The Jensen model available in FLORIS will not be used, as the perturbations lead to an erratic behaviour in the power output.

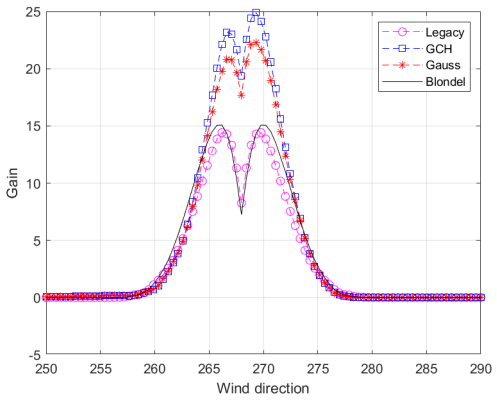

Figure 18: Comparison of power gain for different wind directions.

Note that the wind farm can benefit greatly from wake steering using ESC, regardless of the wake model.
The asymmetry in two of the wake models, are the result of a FLORIS property called *secondary steering*. This property reflects the asymmetry observed in **actual** data, where positive yaw angles are more effective than negative yaw angles. The name secondary steering refers to the fact that the wake from an upstream turbine that is performing wake steering can deflect the wake of a downstream turbine [17].

VI. Conclusion

The findings outlined in this paper show that ESC is a promising control scheme for wind farms. However, further research is needed. Future research should consider the potential effects of the perturbations of the turbines more carefully, for example on maintenance costs or power usage. The effects of noise also need to be researched, as introducing noise into the FLORIS model turned out to be problematic and rarely**(never actually)** converged to a maxima. These downsides might counteract the benefits of wake steering. Furthermore, experimental data from wind tunnels or genuine wind farms is needed to make any claims for the use of ESC on wind farms.

References

[1] M. F. Howland, S. K. Lele, and J. O. Dabiri, "Wind farm power optimization through wake steering," *Proceedings of the National Academy of Sciences*, vol. 116, no. 29, pp. 14 495–14 500, 2019, publisher: National Academy of Sciences _eprint: https://www.pnas.org/content/116/29/14495.full.pdf. [Online]. Available: https://www.pnas.org/content/116/29/14495

[2] "Electricity generation by source." [Online]. Available: https://www.iea.org/data-and-statistics?country=WORLD&fuel=Energy\%20supply&indicator=Electricity\%20generation\%20by\%20source

[3] U. N. Environment, "New report envisages 10-fold increase in global wind power by 2050," Dec. 2019, library Catalog: www.unenvironment.org. [Online]. Available: http://www.unenvironment.org/news-and-stories/story/new-report-envisages-10-fold-increase-global-wind-power-2050

[4] E. Thøgersen, B. Tranberg, J. Herp, and M. Greiner, "Statistical meandering wake model and its application to yaw-angle optimisation of wind farms," *Journal of Physics: Conference Series*, vol. 854, p. 012017, may 2017. [Online]. Available: https://doi.org/10.1088\%2F1742-6596\%2F854\%2F1\%2F012017

[5] M. Ragheb and A. M., *Wind Turbines Theory - The Betz Equation and Optimal Rotor Tip Speed Ratio*. InTech, Jun. 2011. [Online]. Available: http://www.intechopen.com/books/fundamental-and-advanced-topics-in-wind-power/wind-turbines-theory-the-betz-equation-and-optimal-rotor-tip-speed-ratio

[6] N. Jensen, *A note on wind generator interaction*, ser. Risø-M. Risø National Laboratory, 1983, no. 2411.

[7] I. Katic, J. Højstrup, and N. Jensen, "A simple model for cluster efficiency," in *EWEC'86. Proceedings. Vol. 1*, W. Palz and E. Sesto, Eds. A. Raguzzi, 1987, pp. 407–410, european Wind Energy Association Conference and Exhibition, EWEC '86 ; Conference date: 06-10-1986 Through 08-10-1986.

[8] S. Boersma, B. M. Doekemeijer, P. M. O. Gebraad, P. A. Fleming, J. Annoni, A. K. Scholbrock, J. A. Frederik, and J. van Wingerden, "A tutorial on control-oriented modeling and control of wind farms," in *2017 American Control Conference (ACC)*, 2017, pp. 1–18.

[9] NREL, "FLORIS. Version 2.1.1," 2020. [Online]. Available: https://github.com/NREL/floris

[10] M. Bastankhah and F. Porté-Agel, "A new analytical model for wind-turbine wakes," *Renewable Energy*, vol. 70, pp. 116 – 123, 2014, special issue on aerodynamics of offshore wind energy systems and wakes. [Online]. Available: http://www.sciencedirect.com/science/article/pii/S0960148114000317

[11] M. Abkar and F. Porté-Agel, "The effect of atmospheric stability on wind-turbine wakes: A large-eddy simulation study," *Journal of Physics: Conference Series*, vol. 524, p. 012138, jun 2014. [Online]. Available: https://doi.org/10.1088%2F1742-6596%2F524%2F1%2F012138

[12] M. Bastankhah and F. Porté-Agel, "Experimental and theoretical study of wind turbine wakes in yawed conditions," *Journal of Fluid Mechanics*, vol. 806, p. 506–541, 2016.

[13] A. Niayifar and F. Porté-Agel, "Analytical modeling of wind farms: A new approach for power prediction," *Energies*, vol. 9, p. 741, 09 2016.

[14] D. Dilip and F. Porté-Agel, "Wind Turbine Wake Mitigation through Blade Pitch Offset," *Energies*, vol. 10, no. 6, pp. 1–17, May 2017. [Online]. Available: https://ideas.repec.org/a/gam/jeners/v10y2017i6p757-d99940.html

[15] F. Blondel and M. Cathelain, "An alternative form of the super-gaussian wind turbine wake model," *Wind Energy Science Discussions*, vol. 2020, pp. 1–16, 2020. [Online]. Available: https://wes.copernicus.org/preprints/wes-2019-99/

[16] J. King, P. Fleming, R. King, L. Martínez Tossas, C. Bay, R. Mudafort, and E. Simley, "Controls-oriented model for secondary effects of wake steering," 02 2020.

[17] P. Fleming, J. Annoni, M. Churchfield, L. Martínez Tossas, K. Gruchalla, M. Lawson, and P. Moriarty, "A simulation study demonstrating the importance of large-scale trailing vortices in wake steering," *Wind Energy Science*, vol. 3, pp. 243–255, 05 2018.